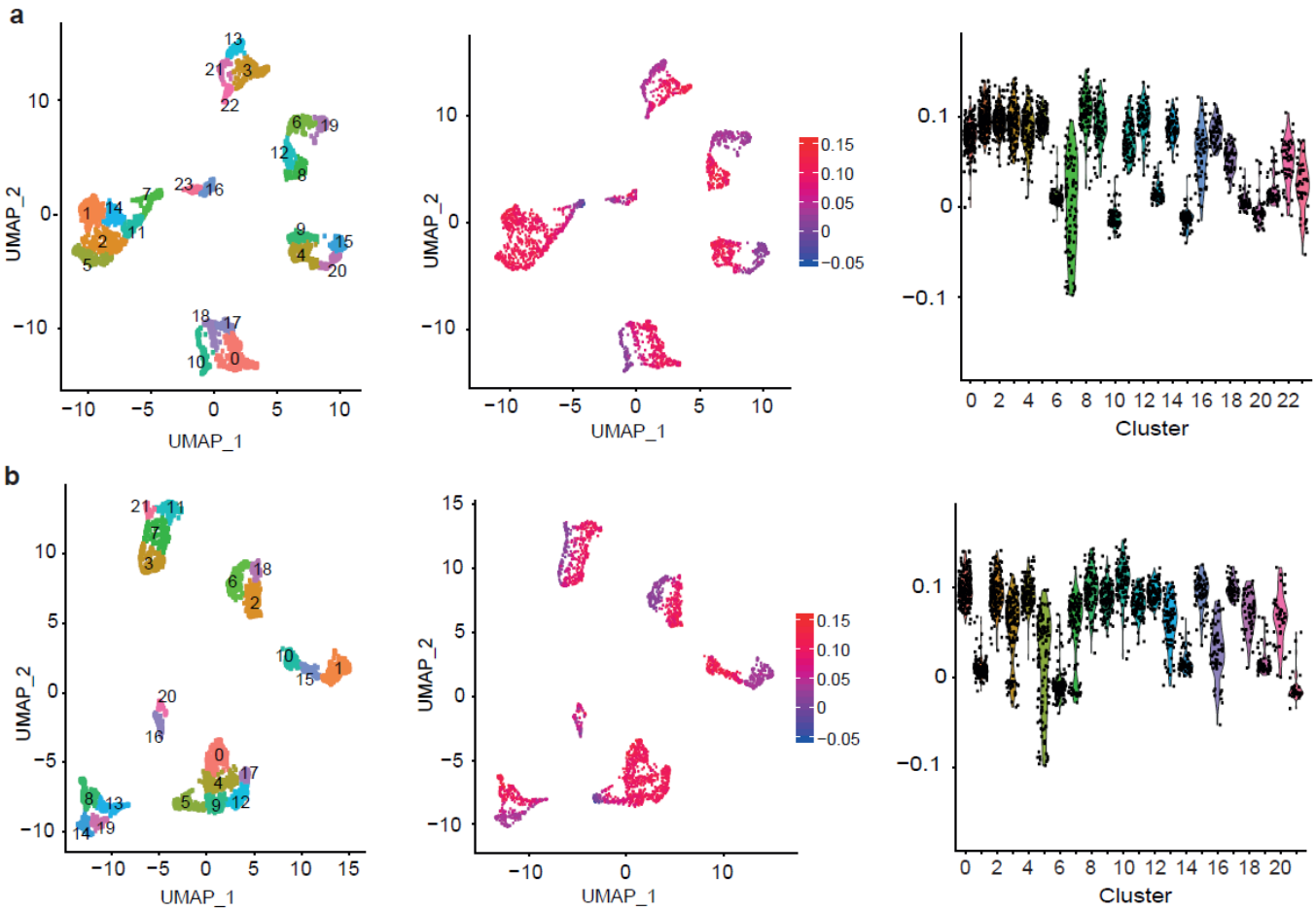

Figure S1: Effect of protoplast isolation (PI) on root scRNA-seq experiment. We reanalyzed the scRNA-seq data from Denyer *et al.*, 2019 without eliminating (a) and eliminating PI-responsive genes (b). The transcriptome of each single cell was correlated with the expression of bulk RNA-seq data from PI roots and non PI root samples from the same study Denyer *et al.*, 2019. Cells with higher correlation with PI samples were not homogeneous distributed in the UMAP plot (a, middle panel), which translated in clusters of cells with different response to PI (a, right panel); the different response to PI was calculated as the difference between the expression correlation of each snRNA-seq transcriptome to bulk RNA-seq data from PI roots minus the correlation to bulk RNA-seq data from non-PI roots (y-axis of right panel plots, and color gradient in the UMAP plots of the middle panel). The same effect was observed when the high PI-responsive genes were eliminated from the analysis (b).

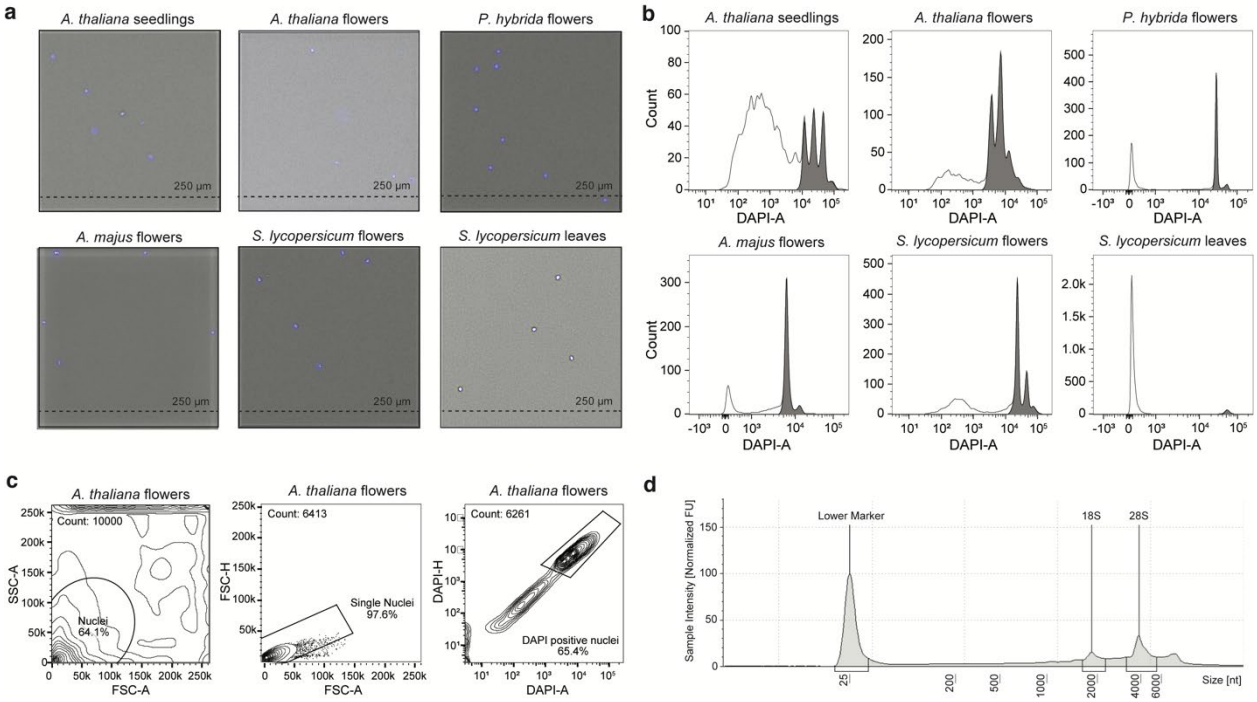

Figure S2: Nuclei isolation quality in different plant tissues/species. a) Microscopy analysis. Sections from disposable Neubauer counting chambers with DAPI stained nuclei after FACS from *Arabidopsis thaliana* seedlings and flowers/inflorescences, *Petunia hybrida* flowers, *Antirrhinum majus* (snapdragon) flowers, *Solanum lycopersicum* (tomato) flowers and leaves. The brightfield images are overlaid with the blue fluorescence images. Images of *Arabidopsis thaliana* samples were captured with a DMi8 microscope by Leica and the others by a BZ-X700 Series microscope by Keyence. The images show that FACS yields clean, debris-free nuclei suspensions irrespective of the initial amount of debris. b) FACS histogram plots of DAPI fluorescent nuclei from different plants and different tissue types are shown after conventional gating for rough debris exclusion and doublet discrimination. The grey filled sections represent the gate that was set for sorting. Different tissue types produce different amounts of nucleus-like sized, low DAPI-fluorescent debris that can only be separated from intact nuclei by gating the high DAPI-fluorescent peaks. c) Gating strategy used for flow cytometry, exemplified for *A.thaliana* inflorescence samples. Nuclei doublets and cell debris are excluded by gating FSC-A *vs* FSC-H and DAPI density. d) Quality control of RNA nuclei samples through electrophoresis-based analysis of RNA derived from sorted nuclei of *A.thaliana* inflorescences.

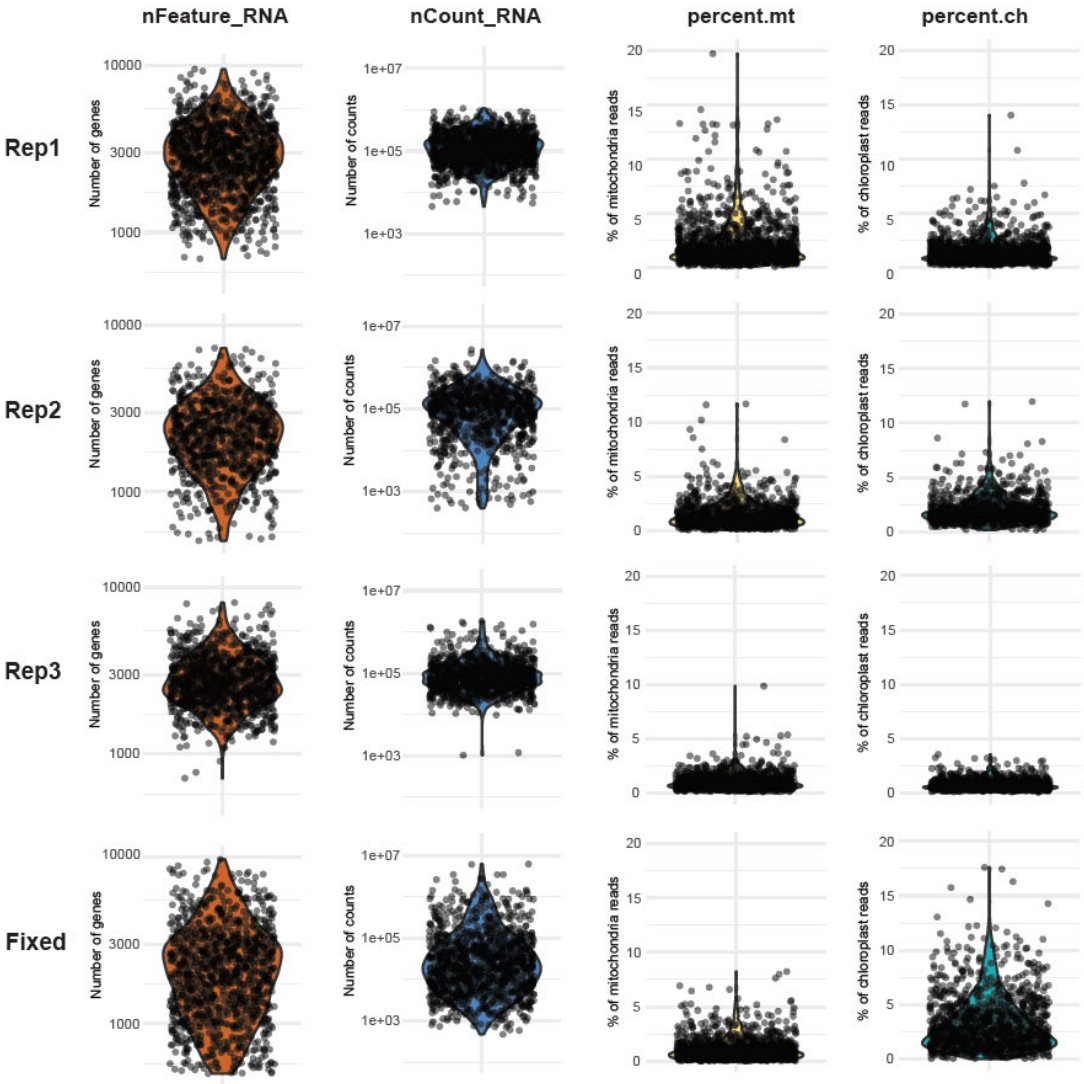

Figure S3: Summary of snRNA-seq seedling datasets. Violin plots showing the total number of detected genes (nFeature_RNA), reads counts (nCount_RNA), the proportion of mitochondria (percent.mt) and chloroplast (percent.ch) per nucleus for each seedling sample.

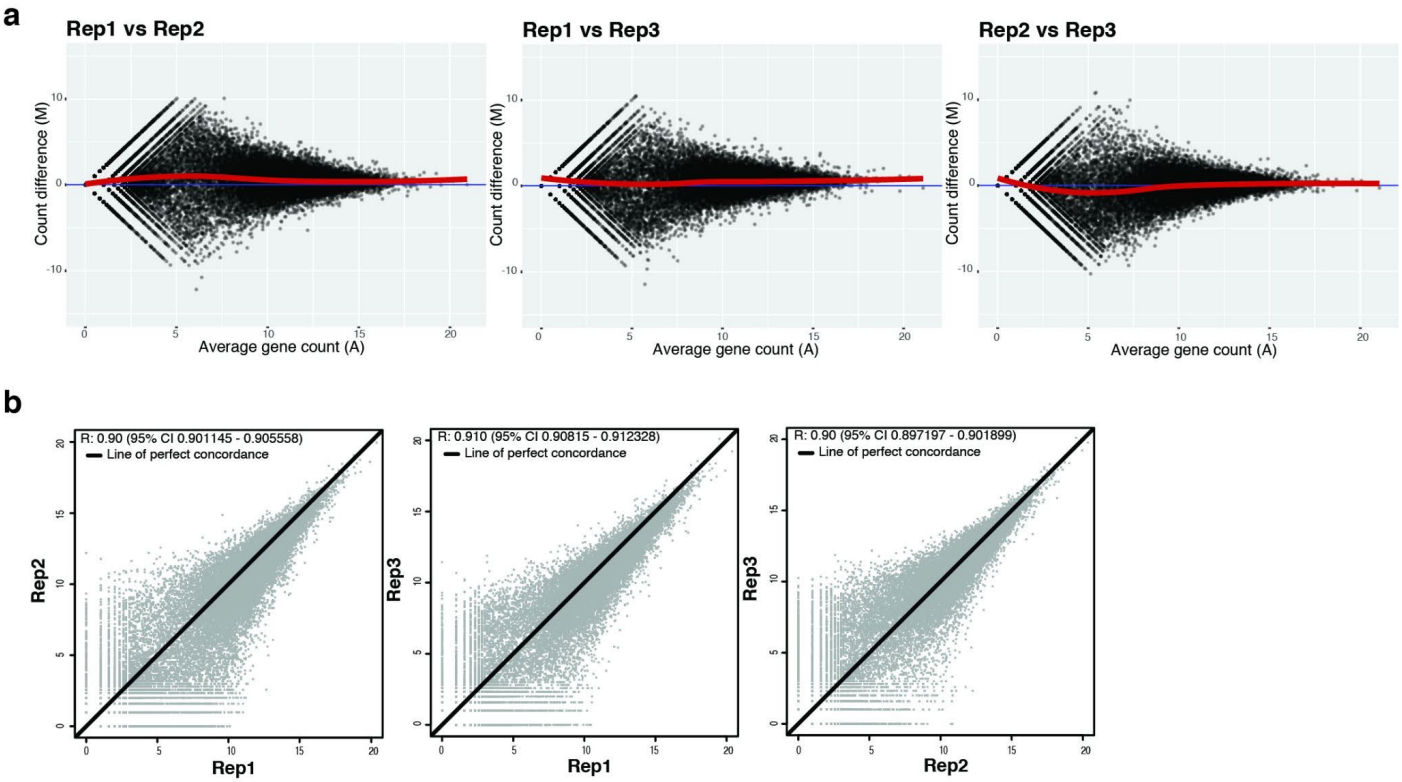

Figure S4: Reproducibility of snRNA-seq. a) MA-plot showing the reproducibility among the biological replicates of the seedling samples. The differences between each pair of replicates was plotted against the average gene count value (A). The red line shows the average differences. b) Pearson's correlation between each pair of replicates.

a

Category	Term	RT	Genes	Count	%	P-Value	Benjamini
GOTERM_CC_DIRECT	chloroplast stroma	RT		485	4.6	3.0E-20	2.0E-17
GOTERM_CC_DIRECT	chloroplast envelope	RT		418	4.0	8.5E-20	2.8E-17
UP_KEYWORDS	Chloroplast	RT		908	8.7	3.7E-17	1.7E-14
UP_KEYWORDS	Plastid	RT		908	8.7	5.4E-16	1.2E-13
UP_KEYWORDS	Photosynthesis	RT		77	0.7	2.6E-14	4.0E-12
GOTERM_CC_DIRECT	chloroplast thylakoid	RT		171	1.6	2.8E-13	6.1E-11
UP_KEYWORDS	Alternative splicing	RT		1732	16.6	1.2E-11	1.4E-9
GOTERM_CC_DIRECT	chloroplast	RT		2078	19.9	8.6E-12	1.4E-9
GOTERM_CC_DIRECT	thylakoid	RT		167	1.6	3.2E-11	4.2E-9
GOTERM_CC_DIRECT	cytosol	RT		1420	13.6	5.1E-11	5.5E-9
UP_KEYWORDS	Transit peptide	RT		1097	10.5	6.1E-11	5.6E-9
GOTERM_CC_DIRECT	apoplast	RT		269	2.6	1.7E-10	1.6E-8
GOTERM_CC_DIRECT	chloroplast thylakoid membrane	RT		264	2.5	3.3E-10	2.7E-8
UP_KEYWORDS	Thylakoid	RT		174	1.7	1.1E-8	8.3E-7
GOTERM_BP_DIRECT	photosynthesis	RT		98	0.9	2.6E-9	6.4E-6
GOTERM_BP_DIRECT	response to cytokinin	RT		137	1.3	4.3E-9	6.4E-6
GOTERM_BP_DIRECT	response to cadmium ion	RT		247	2.4	1.4E-8	1.4E-5
GOTERM_CC_DIRECT	cytosolic ribosome	RT		152	1.5	5.2E-7	3.8E-5
GOTERM_CC_DIRECT	cell wall	RT		300	2.9	1.8E-6	1.2E-4
UP_KEYWORDS	Photosystem II	RT		37	0.4	2.4E-6	1.5E-4
UP_KEYWORDS	Photosystem I	RT		33	0.3	1.4E-5	7.8E-4
GOTERM_CC_DIRECT	vacuole	RT		393	3.8	1.4E-5	8.2E-4
UP_KEYWORDS	Spliceosome	RT		69	0.7	1.7E-5	8.5E-4
UP_KEYWORDS	Phosphoprotein	RT		882	8.4	2.1E-5	9.6E-4
KEGG_PATHWAY	Photosynthesis	RT		39	0.4	1.8E-5	2.4E-3
GOTERM_CC_DIRECT	photosystem II	RT		29	0.3	7.7E-5	4.2E-3
GOTERM_CC_DIRECT	plasmodesma	RT		575	5.5	8.8E-5	4.4E-3
UP_SEQ_FEATURE	transit peptide:Chloroplast	RT		419	4.0	9.7E-7	4.8E-3
GOTERM_CC_DIRECT	nucleolus	RT		282	2.7	1.4E-4	6.7E-3
UP_KEYWORDS	Ribonucleoprotein	RT		302	2.9	2.0E-4	8.3E-3
UP_KEYWORDS	Ribosomal protein	RT		239	2.3	2.2E-4	8.3E-3
KEGG_PATHWAY	Ribosome	RT		214	2.0	1.4E-4	9.0E-3
UP_KEYWORDS	Acetylation	RT		516	4.9	2.7E-4	9.4E-3

b

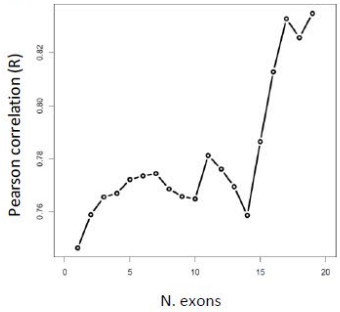

c

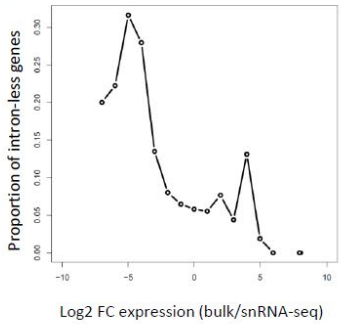

Figure S5: Expression bias of snRNA-seq compared to cytoplasmic bulk RNA-seq. a) Expression differences (DESeq2; FDR<0.05) were detected in the comparison between the 3 replicates of snRNA-seq and the 3 replicates of bulk RNA-seq of seedlings samples. Gene ontology analysis was performed with DAVID (https://david.ncifcrf.gov/). Figure a shows the significant enriched terms (FDR<0.05) found. b) Pearson correlation between snRNA-seq and bulk RNA-seq calculated for the set of genes with a number of exons larger or equal to the value indicated in the x-axis. Expressions of genes with few introns show less agreement between snRNA-seq and bulk RNA-seq than genes with larger number of introns. Correlation was only calculated when there was a minimum number of 200 genes. c) Proportion of genes without introns among the genes showing different log2 FC expression between bulk RNA-seq and snRNA-seq. To group genes, a moving average window was used with size 0.1.

a

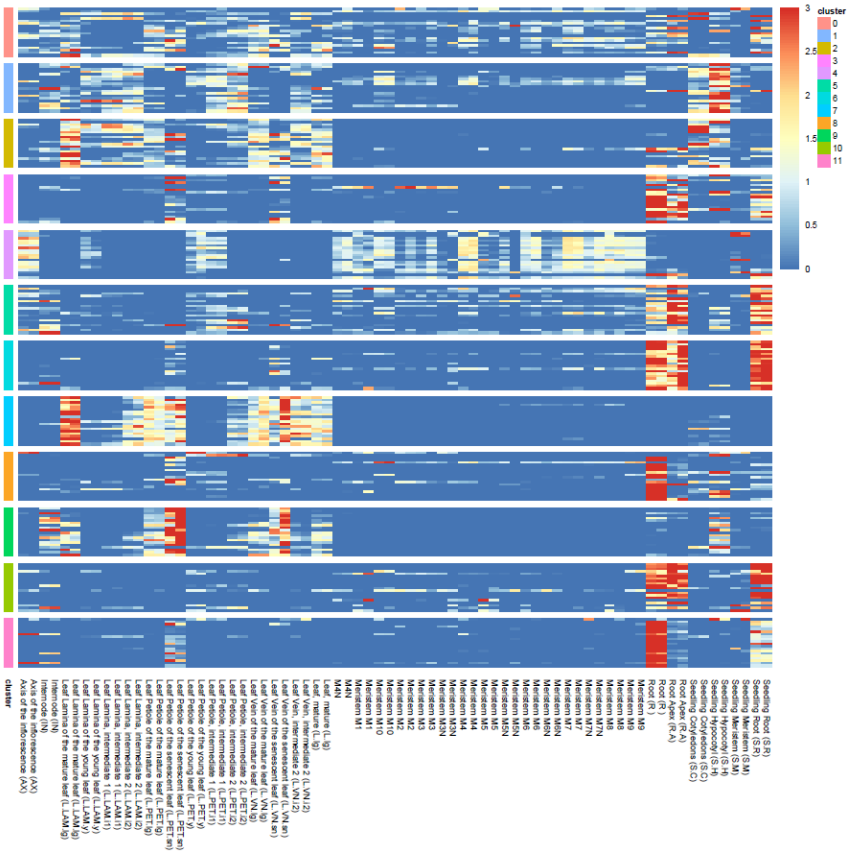
cluster
0
1
2
3
4
5
6
7
8
9
10
11
3
2.5
2
1.5
1
0.5
0
cluster
Intensity (IN)
Axis of the inflorescence (AX)
Axis of the inflorescence (AX)
Leaf Lamina of the mature leaf (L-LAM-g)
Leaf Lamina of the young leaf (L-LAM-y)
Leaf Lamina of the young leaf (L-LAM-y)
Leaf Lamina, intermediate 1 (L-LAM-1)
Leaf Lamina, intermediate 1 (L-LAM-1)
Leaf Lamina, intermediate 2 (L-LAM-2)
Leaf Lamina, intermediate 2 (L-LAM-2)
Leaf Petiole of the mature leaf (L-PET-g)
Leaf Petiole of the mature leaf (L-PET-g)
Leaf Petiole of the senescent leaf (L-PET-sn)
Leaf Petiole of the senescent leaf (L-PET-sn)
Leaf Petiole of the young leaf (L-PET-y)
Leaf Petiole of the young leaf (L-PET-y)
Leaf Petiole, intermediate 1 (L-PET-1)
Leaf Petiole, intermediate 1 (L-PET-1)
Leaf Petiole, intermediate 2 (L-PET-2)
Leaf Petiole, intermediate 2 (L-PET-2)
Leaf Vein of the mature leaf (L-VN-g)
Leaf Vein of the mature leaf (L-VN-g)
Leaf Vein of the senescent leaf (L-VN-sn)
Leaf Vein of the senescent leaf (L-VN-sn)
Leaf Vein, intermediate 2 (L-VN-2)
Leaf Vein, intermediate 2 (L-VN-2)
Leaf, mature (L-g)
Leaf, mature (L-g)
M4N
M4N
Meristem M1
Meristem M1
Meristem M10
Meristem M10
Meristem M2
Meristem M2
Meristem M3
Meristem M3
Meristem M3N
Meristem M3N
Meristem M4
Meristem M4
Meristem M5
Meristem M5
Meristem M5N
Meristem M5N
Meristem M6
Meristem M6
Meristem M6N
Meristem M6N
Meristem M7
Meristem M7
Meristem M7N
Meristem M7N
Meristem M8
Meristem M8
Meristem M9
Meristem M9
Root Apex (R-A)
Root Apex (R-A)
Root Apex (R-A)
Root Apex (R-A)
Root (R-)
Root (R-)
Seeding Cotyledons (S-C)
Seeding Cotyledons (S-C)
Seeding Hypocotyl (S-H)
Seeding Hypocotyl (S-H)
Seeding Meristem (S-M)
Seeding Meristem (S-M)
Seeding Root (S-R)
Seeding Root (S-R)

b

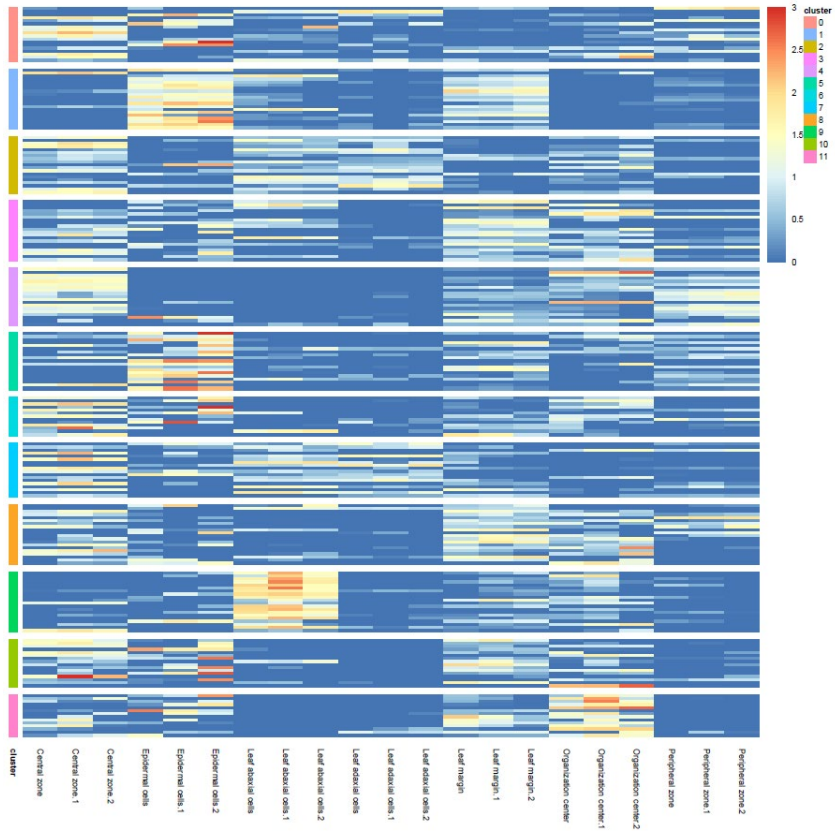
cluster
0
1
2
3
4
5
6
7
8
9
10
11
3
2.5
2
1.5
1
0.5
0
cluster
Central zone
Central zone 1
Central zone 2
Epidermal cells
Epidermal cells 1
Epidermal cells 2
Leaf adaxial cells
Leaf adaxial cells 1
Leaf adaxial cells 2
Leaf adaxial cells
Leaf adaxial cells 1
Leaf adaxial cells 2
Leaf margin
Leaf margin 1
Leaf margin 2
Organization center
Organization center 1
Organization center 2
Peripheral zone
Peripheral zone 1
Peripheral zone 2

Figure S6: Annotation of seedling clusters using TraVaDB (a) and shoot apical meristem (Tian *et al.*, 2019) domains (b). Heatmaps showing the expression level of the top 20 gene markers from each cluster in tissue- specific transcriptome datasets.

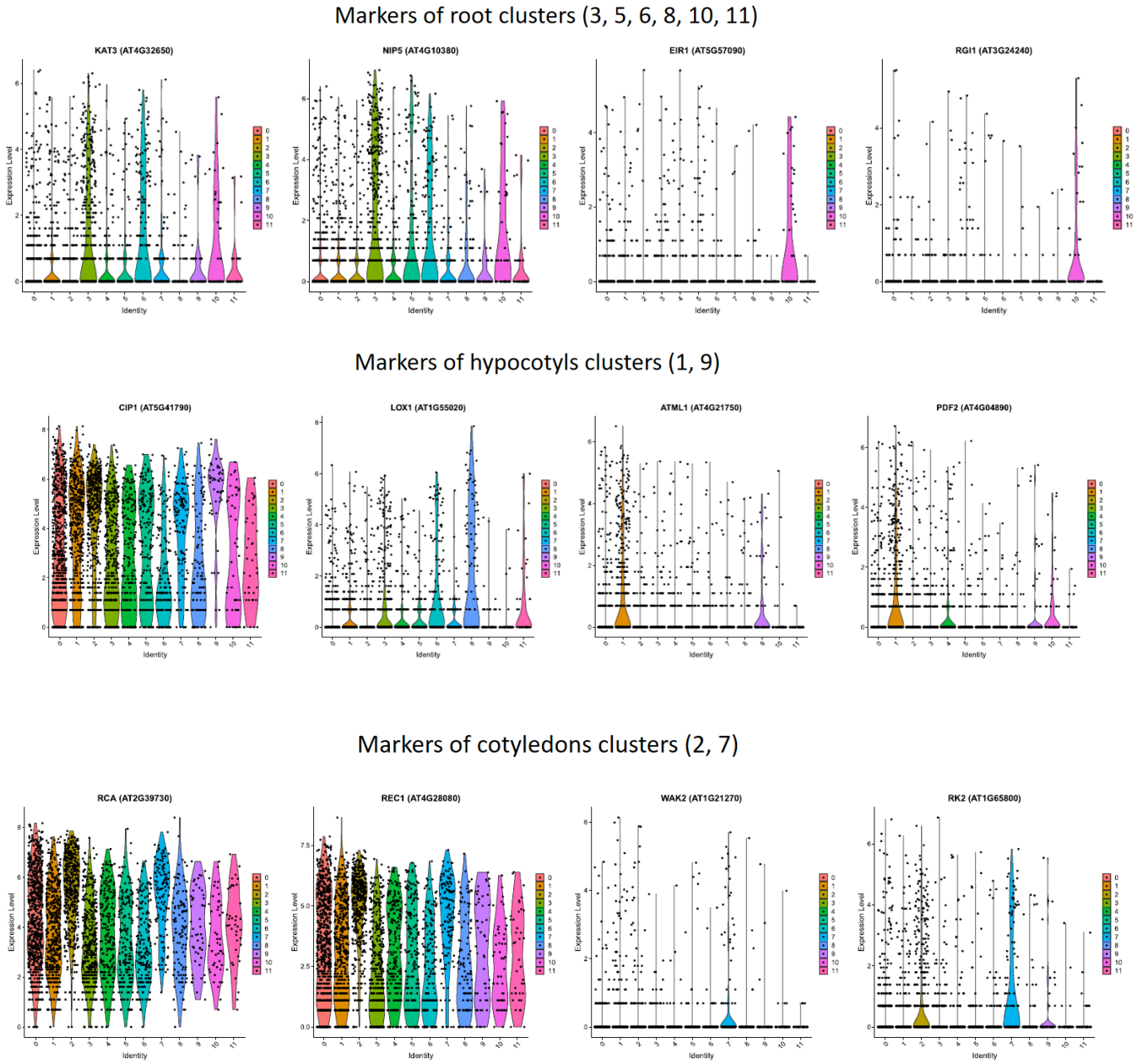

Figure S7. Gene expression of representative seedling marker genes.

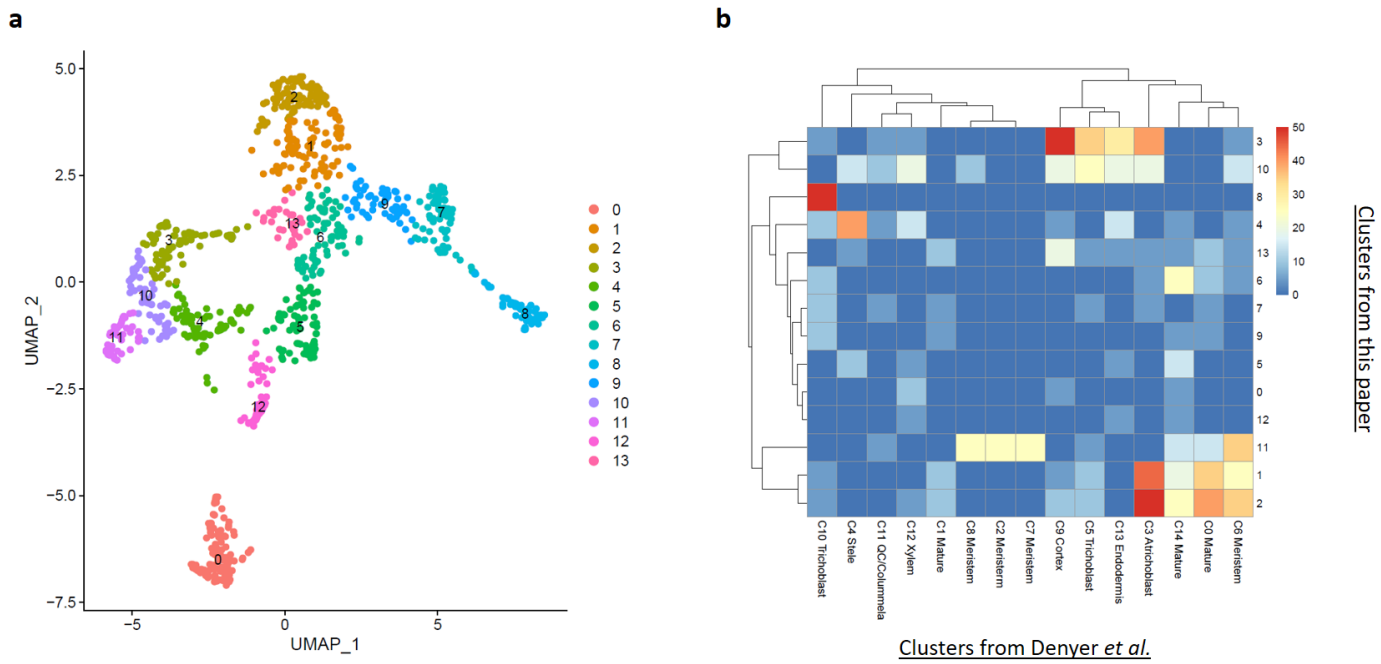

Figure S8: Analysis of a subset of root nuclei derived from snRNA-seq seedling dataset. a) UMAP of 14 clusters (n=980 nuclei). b) Proportion of markers overlapping the top 500 markers found by Denyer *et al.*, 2019. Proportion values bigger than 50% were set to 50% for visualization purpose.

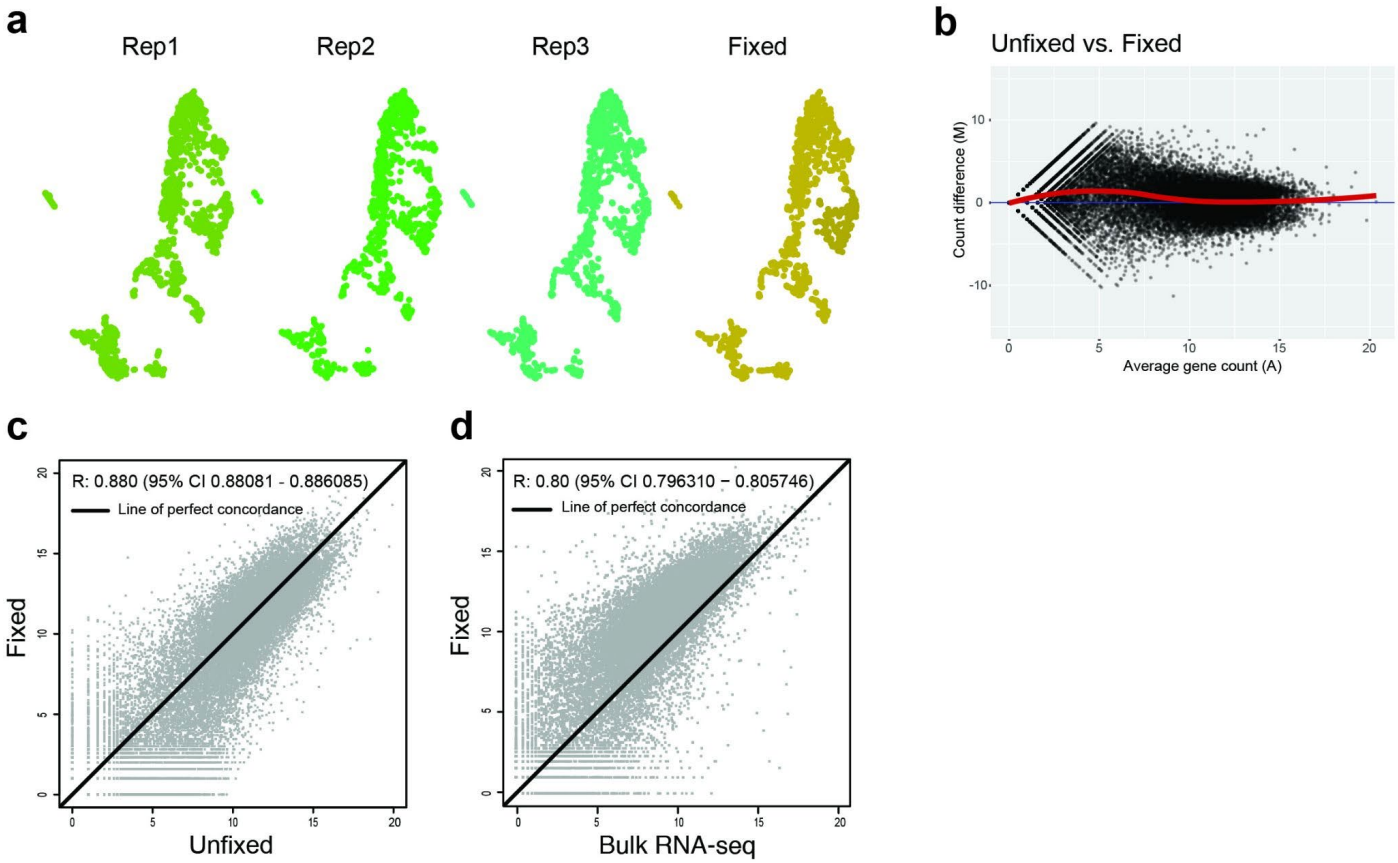

Figure S9: Correlation between fixed and unfixed seedling replicates and between fixed and bulk RNA-seq replicates. a) UMAP plot showing similar nuclei distribution of fixed and unfixed seedling replicates. b) MA-plot showing the similarity between fixed and the average of the 3 unfixed replicates. c) Pearson's correlation between fixed and the average of the 3 unfixed replicates (R= 0.88). d). Pearson's correlation between fixed and the average of the 3 bulk RNA-seq replicates (R= 0.80).

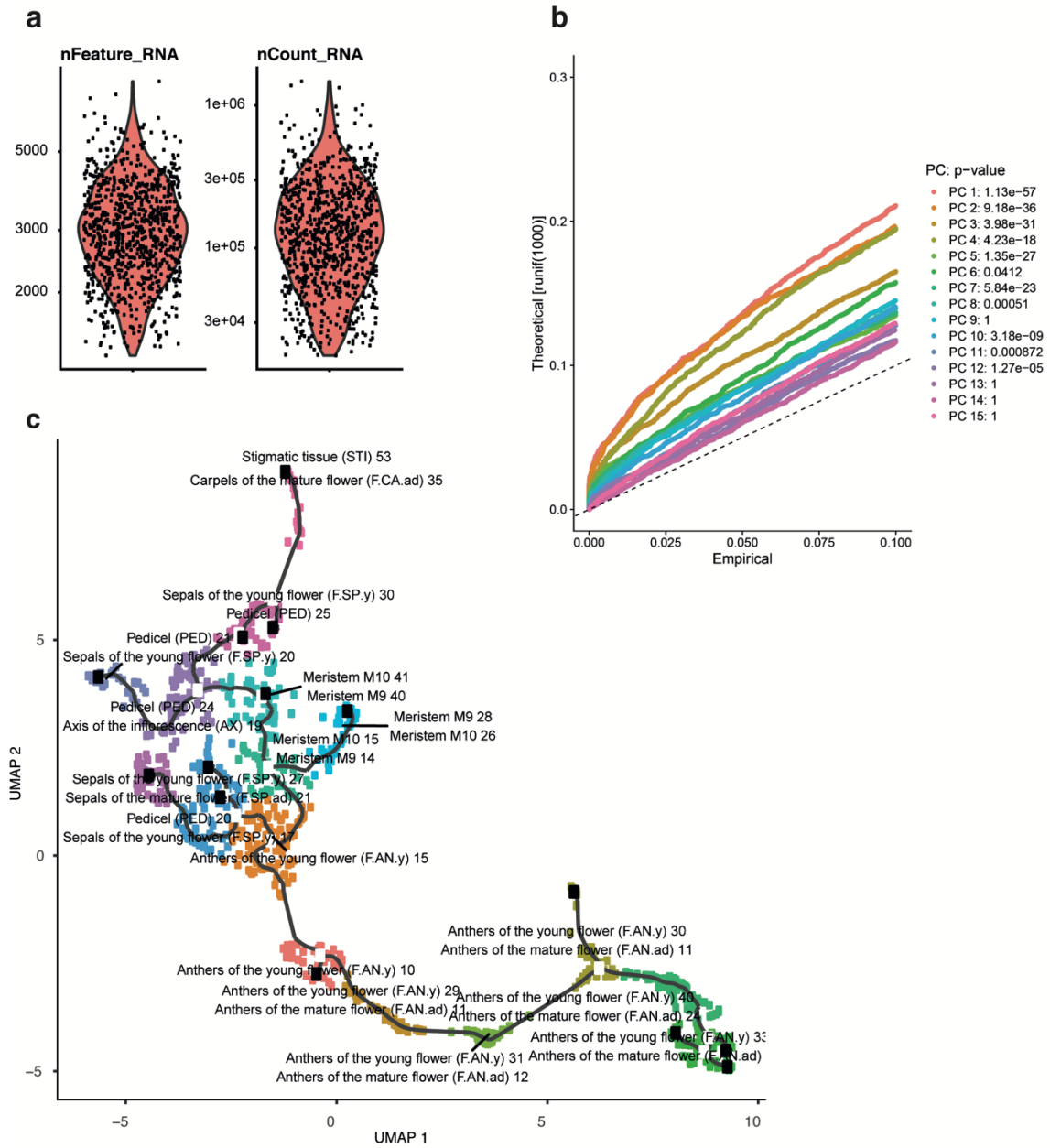

Figure S10: Single-nuclei transcriptome analysis of *A.thaliana* flower development. a) Number of genes per nucleus (nFeature) and a number of reads per gene (nCount) after filtering using Seurat. b) JACKSTRAW plot to identify the optimal number of PCAs for the analysis of the inflorescence dataset. c) Annotation of clusters based on correlation: the average gene expression of each cluster was correlated (Spearman) against each one of the TraVaDB transcriptome datasets considered. The two labels plotted on top of each cluster indicate the two TraVaDB samples with the highest correlation, the number indicates the Rho coefficient *100.

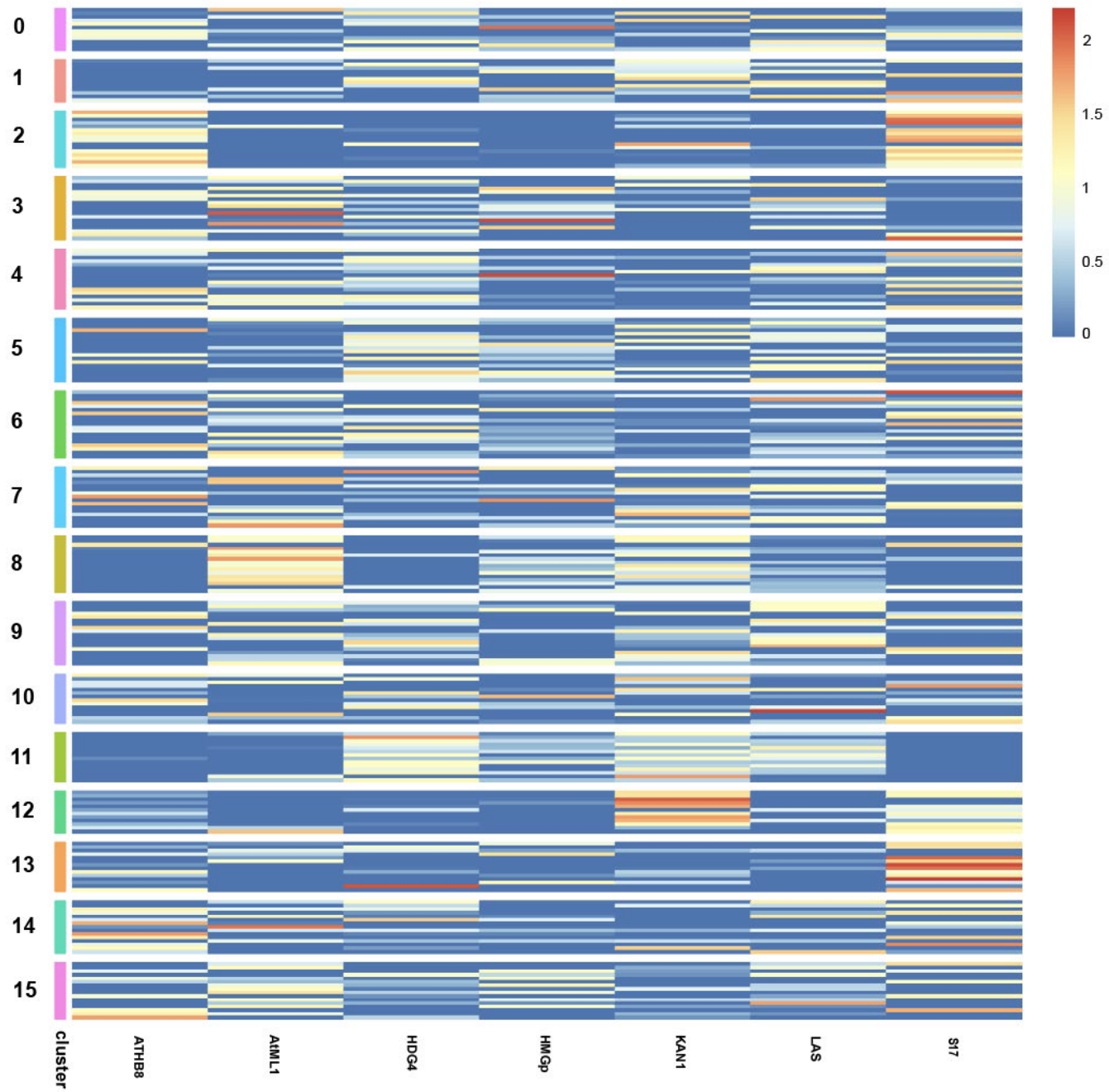

Figure S11: Annotation of flower clusters using cell-specific shoot apical meristem population bulk RNA-seq dataset (Yadav *et al.*, 2014). Heatmap showing the expression level of the top 20 gene markers from each cluster in cell-specific shoot apical meristem population transcriptomes. Following Yadav *et al.*, *ATML1* promoter labels the L1 layer, *HDG4*: the L2 layer, *S17*: the phloem, *AtHB8*: the procambial cells, *KAN1*: the outer edges of the peripheral zone, *LAS*: organ boundaries, and *HMG* promoter to label meristematic L1 layer cells.

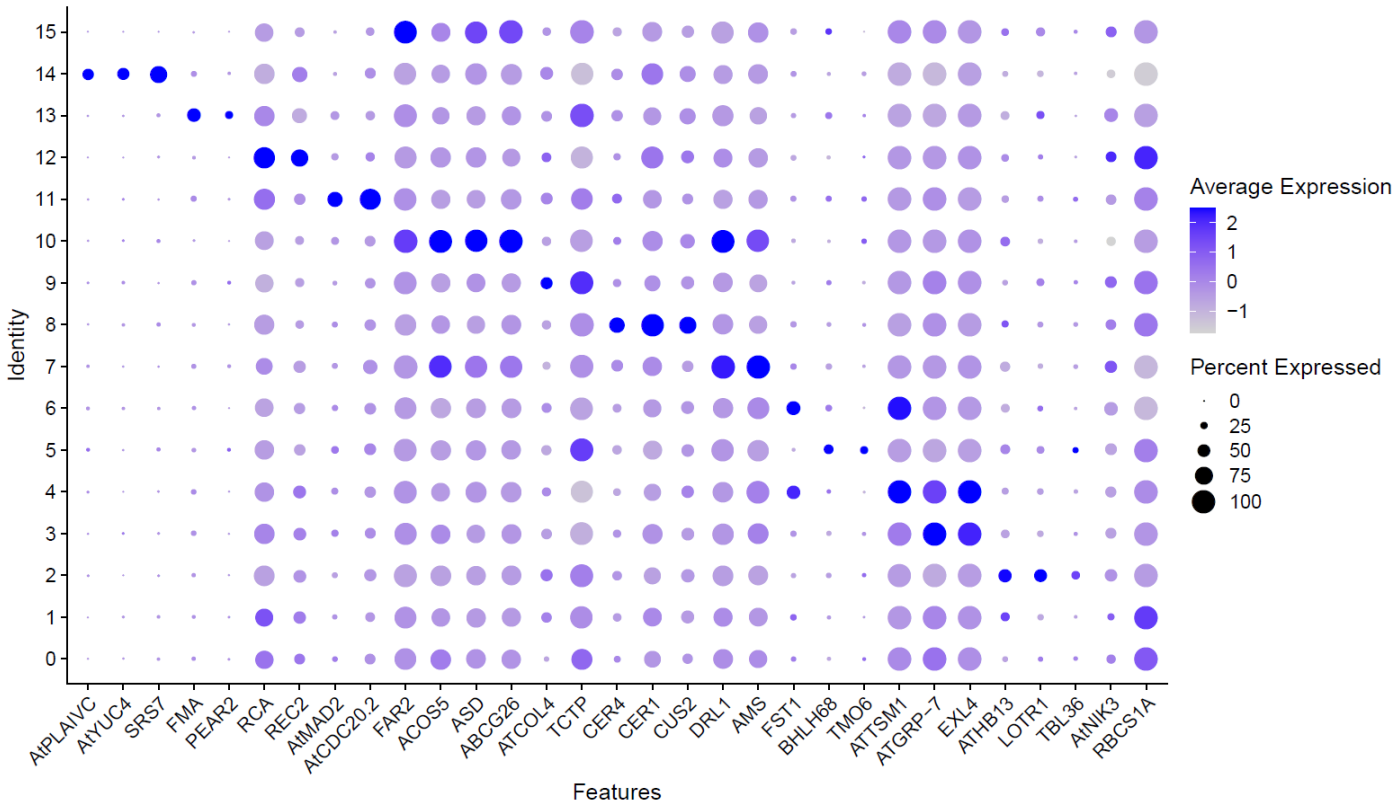

Figure S12: Expression of selected marker genes of flower with known function.

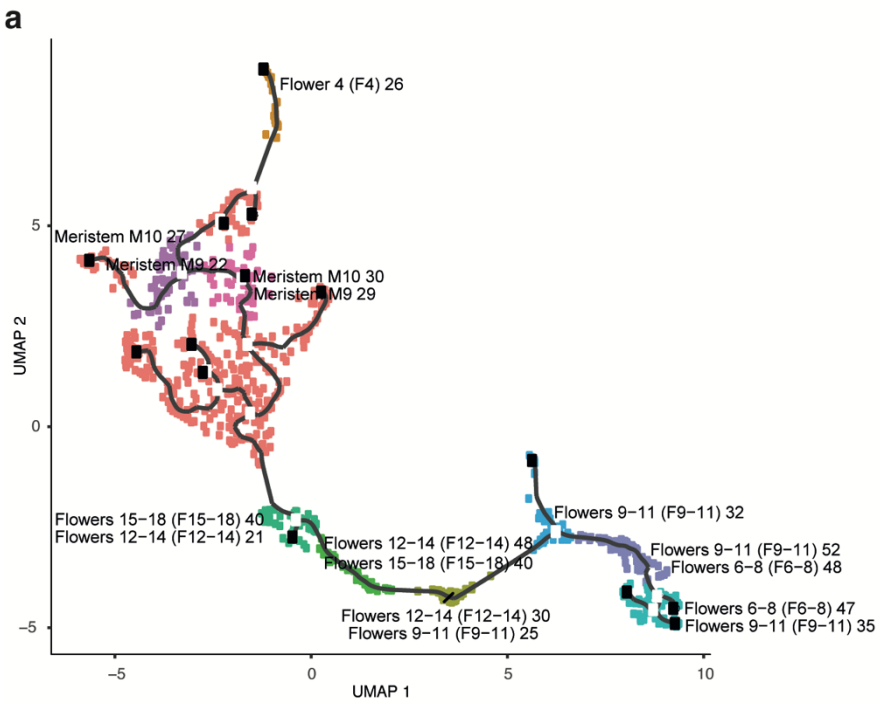
a
Flower 4 (F4) 26
Meristem M10 27
Meristem M9 22
Meristem M10 30
Meristem M9 29
Flowers 15–18 (F15–18) 40
Flowers 12–14 (F12–14) 21
Flowers 12–14 (F12–14) 48
Flowers 15–18 (F15–18) 40
Flowers 12–14 (F12–14) 30
Flowers 9–11 (F9–11) 25
Flowers 9–11 (F9–11) 32
Flowers 9–11 (F9–11) 52
Flowers 6–8 (F6–8) 48
Flowers 6–8 (F6–8) 47
Flowers 9–11 (F9–11) 35
UMAP 1
UMAP 2

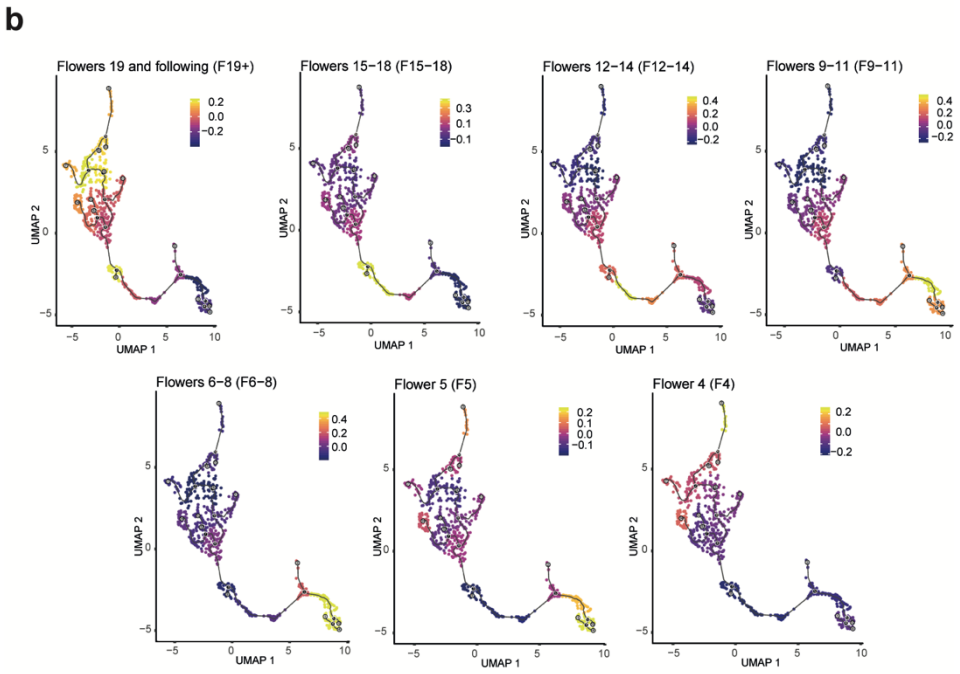
b
Flowers 19 and following (F19+)
Flowers 15–18 (F15–18)
Flowers 12–14 (F12–14)
Flowers 9–11 (F9–11)
Flowers 6–8 (F6–8)
Flower 5 (F5)
Flower 4 (F4)
UMAP 1
UMAP 2

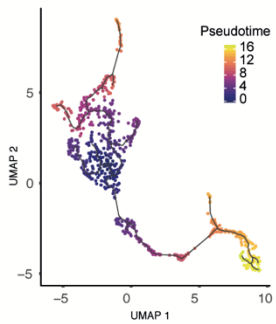
c
Pseudotime
UMAP 1
UMAP 2

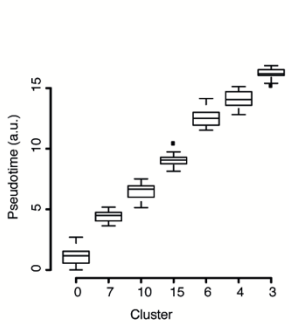
d
Pseudotime (a.u.)
Cluster

Figure S13: Temporal trajectory of the floral snRNA-seq dataset. a) Annotation of clusters based on the correlation with the "Flower stages" samples in the TraVaDB dataset: the average gene expression of each cluster was correlated against the TraVaDB transcriptome datasets considered. The two labels plotted on top of each cluster indicate the two TraVaDB samples with the highest correlation, the number indicates the Rho coefficient *100, only Rho coefficients bigger than 0.2 are shown. The black line indicates the pseudotime trajectory predicted by Monocle3. b) To extend figure a, the Spearman's correlation coefficient (Rho) of each cluster against the different "Flower stage" samples from TraVaDB is shown on the UMAP representation of the data, the title of the data indicates which TraVaDB sample the snRNA-seq data was correlated. The graph shows that the temporal order of anthers clusters by developmental stage from early to late predicted by the annotation using TraVaDB is: 0, 7, 10,15, 6, 4 and 3. c) UMAP plot showing the predicted pseudotime by Monocle3, being 0 the earliest time point; cluster 0 (meristem/early anther) was considered the earliest stage in this analysis. d) Boxplot showing the distribution of pseudotime of the cells belonging to anthers clusters. Clusters were ordered by developmental stages predicted by the overlap with TraVaDB. The graph shows the good agreement of the predicted developmental time by TraVaDB and pseudotime.

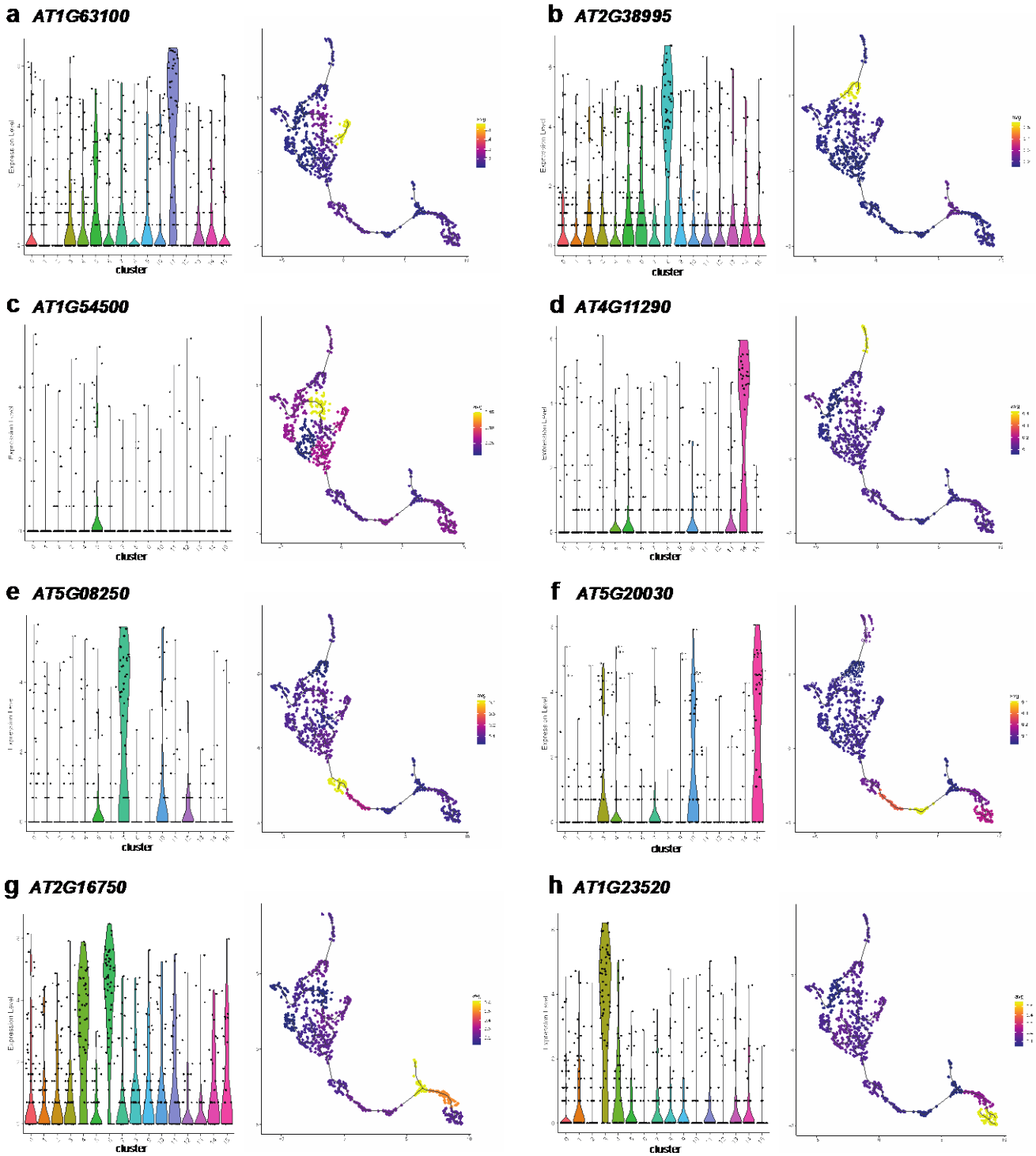

Figure S14. Gene expression of the validated marker genes of flowers illustrated in Figure 3.

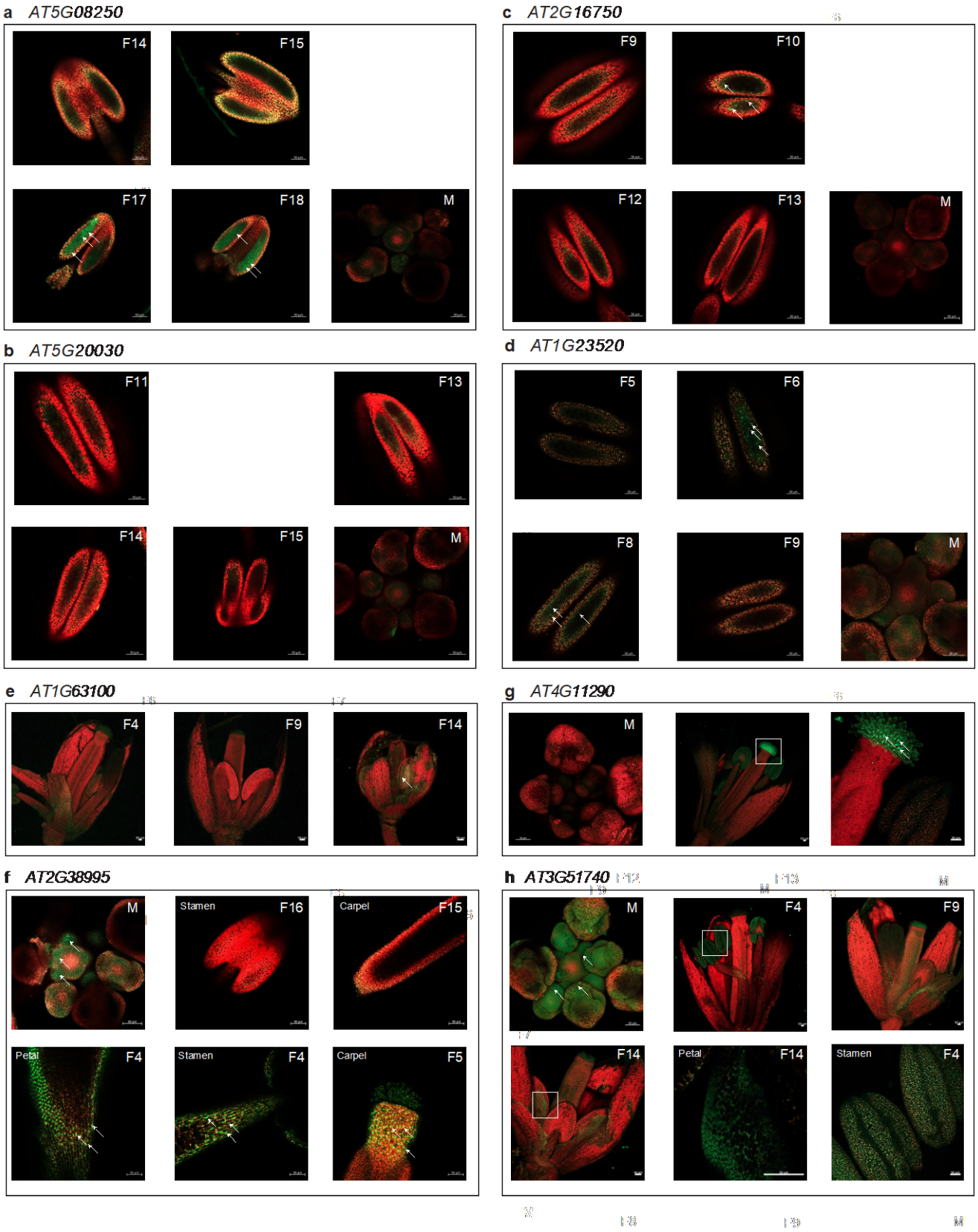

Figure S15: Validation of cluster-specific marker genes of flowers with transcriptional reporter lines. Confocal images of GFP reporter lines: a) *AT5G08250*, flower 14,15,17,18 and meristem. b) *AT5G20030*, flower 11, 13, 14, 15 and meristem; c) *AT2G16750*, flower 9, 10, 12, 13 and meristem. d) *AT1G23520*, flower 5, 6, 8, 9 and meristem. e)

AT1G63100, flower 4, 9, 14. f) *AT2G38995*, meristem, anther of flower 16, carpel of flower 15 and flower 5, petal and stamen filament of flower 4. g) *AT4G11290*, meristem, all four organs in one flower and enlarged picture showing carpel and stamen from the highlighted region in the white square. h) *AT3G51740,* meristem, flower 4, 9, 14 and enlarged pictures showing the autofluorescence of petals and stamens from the highlighted regions in the white squares. White arrowheads indicate exemplary GFP signals. Flower numbers are according to TraVaDB. Scale bars, 50 μm.